GEOPHYSICS, VOL. 50, NO. 1 (JANUARY 1985); P. 63–76, 12 FIGS., 4 TABLES

Velocity determination in layered systems with arbitrarily curved interfaces by means of wave field extrapolation of CMP data

C. P. A. Wapenaar* and A. J. Berkhout*

ABSTRACT

The paper starts with a brief review of conventional velocity determination procedures for plane-layered systems. These methods assume hyperbolic moveout curves in common midpoint (CMP) data. It is shown that in layered systems with arbitrarily curved interfaces these methods fail since the moveout curves are nonhyperbolic. The subject of this paper is a wave-theoretical approach to velocity determination. By means of wave field extrapolation of CMP data, nonhyperbolic moveout curves are transformed into hyperbolic ones. The proposed process is called velocity replacement (VR) since an inhomogeneous overburden is replaced by a homogeneous velocity medium. The effect of VR is illustrated on synthetic data. From the results it may be concluded that velocity determination after VR yields significantly more accurate results than velocity determination before VR. The technique of VR is also proposed as a preprocessing tool prior to stack in situations of nonhyperbolic moveout curves.

INTRODUCTION

Generally, the seismic velocity is a function of all three subsurface coordinates. However, most seismic processing methods assume, within restricted lateral dimensions, a layered velocity model, i.e., the velocity is constant within an arbitrarily shaped layer (Figure 1). For many geologic situations this is a reasonable assumption. For such a layered system Durbaum (1954) showed that the traveltime $T_N(x)$ of a seismic pulse reflected by the Nth subsurface reflector (i.e., interface between layer N and layer $N+1$), generated and registered with a source-receiver separation (offset) x can be written as an infinite MacLaurin series:

$$T_N^2(x) = \sum_{k=0}^{\infty} A_{N,k} x^k. \qquad (1)$$

The coefficients $A_{N,k}$ are related to interval velocities, layer thicknesses, and reflector shapes (i.e., dip and curvature). For a horizontally layered system Dix (1955) approximated relation (1) for small offsets x by a hyperbolic relation where only the coefficients $A_{N,0}$ and $A_{N,2}$ are nonzero. Coefficients $A_{N,0}$ and

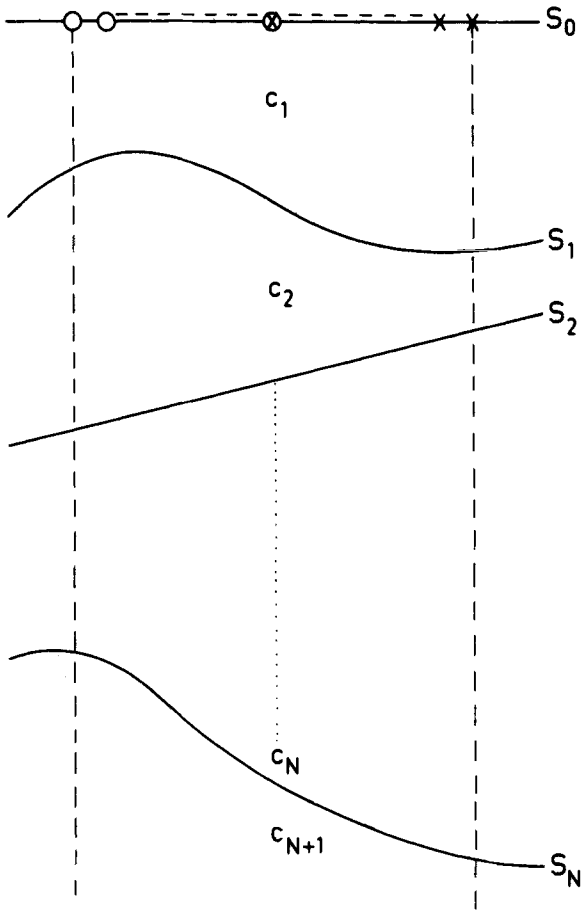

FIG. 1. The basic configuration in most seismic processing methods is a layered subsurface with a constant velocity in each layer within restricted lateral dimensions.

Presented at the 53rd Annual International SEG Meeting, September 12, 1983, in Las Vegas. Manuscript received by the Editor September 20, 1982; revised manuscript received July 25, 1984.
*Delft University of Technology, Lab, Applied Physics, Group of Acoustics, P. O. Box 5046, 2600 GA Delft, The Netherlands

$A_{N,2}$ are related to the seismic parameters zero-offset (ZO) traveltime $T_N(0)$ and normal moveout (NMO) velocity C_N, respectively. Taner and Koehler (1969) showed that, assuming hyperbolic moveout curves, $T_N(0)$ and C_N can be derived from offset data. The numerical method they proposed is based on the evaluation of a two-dimensional (2-D) coherence function (velocity spectra) whose maxima refer to C_N and $T_N(0)$ for all N. De Vries and Berkhout (1982) use a minimum entropy criterion to focused CMP data in order to determine NMO velocities. Dix solved the inverse problem: that is derivation of interval velocities and layer thicknesses from NMO velocities C_N and ZO traveltimes $T_N(0)$. For the first layer ($N = 1$) this method is exact. For a specific offset data arrangement, common midpoint data (CMP), small reflector dips may be included. Among others, Cook (1967) showed that application of Dix's method in areas of gentle dips (less than 5 degrees), yields interval velocities 2 percent to 3 percent higher than actually measured in well-velocity surveys. Also for CMP data, Larner and Rooney (1972) approximated relation (1) by a hyperbolic relation for the arbitrary dipping plane-layer case. Shah (1973) derived the same relation by studying the radius of curvature of a wavefront propagating through a plane-layered system. Hubral (1976) developed a method to solve the inverse problem for the 3-D dipping plane-layer case. Krey (1976) discussed the validity of the hyperbolic traveltime/offset relation for systems with curved interfaces. Particularly in the latter situation, very small offsets must be assumed. Lynn and Claerbout (1982) developed a hyperbolic relation for systems with arbitrary lateral velocity variations by taking into account the lateral derivatives of the medium velocity.

Another approach to velocity determination in the dipping plane-layer case is based on τ, p mapping of CMP data, among others described by Diebold and Stoffa (1981). In this method CMP data in the traveltime/offset domain (T, x) are mapped into the intercept-time/ray-parameter domain (τ, p) where the velocity determination is performed. The intercept-time/ray-parameter relation is elliptical. Since this relation is exact for horizontally layered systems, also wide-offset data (including refracted and post-critically reflected data) can be handled by this velocity determination procedure.

The success of the methods discussed so far is based on the fact that for simple configurations the infinite series (1) may be approximated by a hyperbolic relation defined by only two coefficients. Also the ellipses in the (τ, p)-domain are defined by two coefficients only. However, in arbitrarily layered systems *nonhyperbolic* moveout curves occur and more than two terms of the MacLaurin series are required to approximate the traveltime/offset relation, particularly when offsets are not small.

Several velocity determination procedures have been developed, taking into account the nonhyperbolic character of the moveout curves. May and Straley (1979) incorporated higher-order terms in the traveltime/offset relation. Their method becomes impractical for approximations higher than fourth order. Gjøystdal and Ursin (1981) and Vander Made et al. (1984) developed reflection-time inversion methods for complex inhomogeneous media, based on parameter estimation. They dropped the concept of stacking along moveout curves. Instead, a peak-picking algorithm is required in these methods.

The method introduced in this paper is based on preprocessing of CMP data in such a way that the traveltime/offset relation in the processed CMP data may be closely approximated by a hyperbolic relation. This situation is obtained by transforming the inhomogeneous layered system into a homogeneous system, which is realized by replacing the different velocities in the successive layers by one constant velocity. This process, velocity replacement (VR), is based on forward and inverse wave field extrapolation of CMP data. Although the restriction is not fundamental, we will assume 2-D subsurface configurations.

In the literature several velocity determination procedures based on wave theory are given. Gardner et al. (1974) and Sattlegger (1975) showed how the migration velocity can be determined by optimizing a nonrecursive prestack migration output. Yilmaz and Chambers (1980) used wave-field extrapolation to perform NMO correction in order to resolve strongly interfering events. In all these methods hyperbolic moveout curves are assumed, nonhyperbolic moveout curves are not transformed into hyperbolic ones. Doherty and Claerbout (1976) used a finite-difference technique in order to downward continue seismic records (by means of inverse wave field extrapolation) as a preprocessor for conventional velocity estimation techniques. Since receivers only are downward continued, nonhyperbolic moveout curves are only partly transformed into hyperbolic ones. In our method conventional velocity estimation techniques are used after independent processing of CMP gathers: *nonhyperbolic* moveout curves are transformed into *hyperbolic* ones.

Summarizing, for inhomogeneous systems the traveltime/offset relation is generally complicated and advanced techniques are required to recover all coefficients in this relation. To simplify the procedure two approaches may be followed.

(1) For simple configurations the infinite MacLaurin series, which describes the traveltime/offset relation for CMP data, may be approximated by two terms (hyperbolic assumption). The two coefficients are easily found from coherence calculations. Applications: horizontally layered systems, dipping plane layered systems, layered systems with curved interfaces assuming very small offsets and/or small velocity variations.

(2) For more complicated configurations the system can be made homogeneous by a wave-theory based velocity replacement technique. After application the traveltime/offset relation can be described again by two terms only. Application: Layered systems with arbitrarily curved interfaces, without assuming serious restrictions on offset and/or velocity variations.

Next we discuss briefly some well-known moveout curve approximation methods (1) which can be regarded as an introduction to our moveout curve transformation method (2), described in the second part of the paper.

CONVENTIONAL VELOCITY DETERMINATION PROCEDURES

In this section we summarize some important conventional velocity determination procedures which are based on the hyperbolic assumption. We first study the two-term approximation of relation (1) for the CMP configuration in the dipping

plane-layer case. Since our research concerns 2-D configurations only, we restrict ourselves to 2-D situations.

Consider the configuration shown in Figure 2. According to Larner and Rooney (1972) and Shah (1973) the traveltime $T_N(x)$ for reflection N, given by relation (1), may be approximated for small offsets x by a hyperbolic relation

$$T_N^2(x) \approx A_{N,0} + A_{N,2}x^2 = T_N^2(0) + \frac{x^2}{C_N^2}, \tag{2a}$$

where

$$T_N(0) = \sum_{n=1}^{N} \Delta T_n, \tag{2b}$$

and

$$C_N^2 = \frac{1}{T_N(0)\cos^2\psi_0} \sum_{n=1}^{N} \prod_{k=0}^{n-1} \left(\frac{\cos^2\psi_k'}{\cos^2\psi_k}\right) c_n^2 \Delta T_n, \tag{2c}$$

with

C_N = NMO velocity for reflection N,
$T_N(0)$ = total two-way zero-offset (ZO) traveltime between the surface and reflector N,
c_n = interval velocity in layer n,
ΔT_n = two-way interval ZO traveltime in layer n,
ψ_0 = emergence angle of ZO raypath at surface,
$\psi_0' = \psi_0$,
ψ_k = refraction angle of ZO raypath at the kth interface,
and
ψ_k' = incidence angle of ZO raypath at the kth interface.

For $N = 1$ relation (2) is exact. For horizontally layered systems relation (2) reduces to the well-known Dix relation (Dix, 1955), ($\psi_k = \psi_k' = 0$ for all k). In this case the NMO velocity C_N equals the rms velocity (effective velocity) between the surface and reflector N

$$C_N^2 = \frac{1}{T_N(0)} \sum_{n=1}^{N} c_n^2 \Delta T_n. \tag{3}$$

The seismic parameters C_N and $T_N(0)$ for all N can be derived from CMP data. We will not discuss this item but refer the interested reader to Taner and Koehler (1969).

Hubral (1976) developed a method, based on relation (2), to derive interval parameters (interval velocity, layer thickness, and reflector dip) from surface measurements. Since three interval parameters must be determined for each layer [apart from C_N and $T_N(0)$] additional information is required. From $T_N(0)$ values of adjacent CMP gathers the time dip $dT_N(0)/dx'$ can be derived. The time dip is the first derivative of the ZO traveltime with respect to the lateral midpoint position x' and is represented by a dip in the x', t-diagram of the ZO time series. For plane layers and constant interval velocities $dT_N(0)/dx'$ is constant; for horizontal layers $dT_N(0)/dx'$ equals zero. From the time dip for reflection N and the interval velocity in the first layer, the emergence angle ψ_0 at the surface of ZO raypath N can be calculated with Tuchel's formula (Tuchel, 1943)

$$dT_N(0)/dx' = 2 \sin\psi_0/c_1. \tag{4}$$

Assuming layers 1 through $N-1$ are reconstructed, the interval parameters for layer N can be obtained as follows.

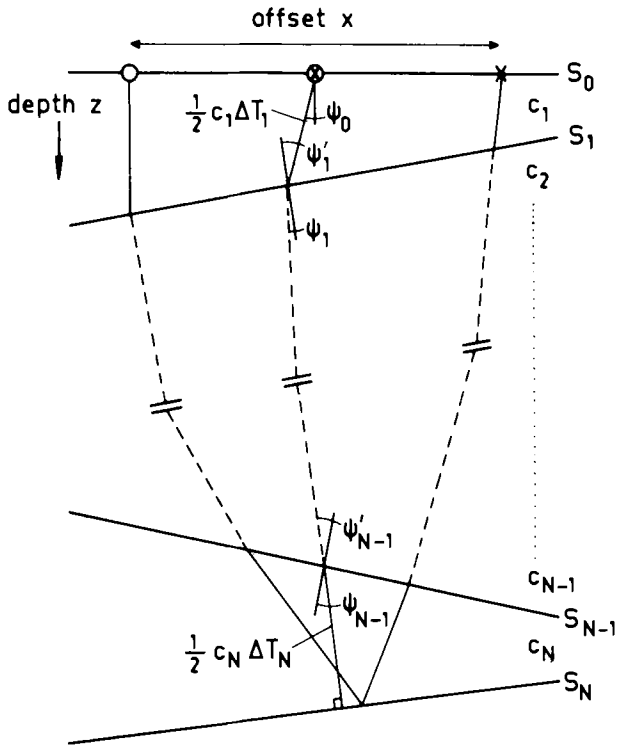

FIG. 2. Dipping plane layered system. For the CMP configuration the traveltime $T_N(x)$ for reflection N and offset x is approximately given by relation (2).

(1) Derive C_N and $T_N(0)$ for reflection N from CMP data by means of coherence calculations.
(2) Derive $dT_N(0)/dx'$ for reflection N from $T_N(0)$ values of adjacent CMP gathers.
(3) Trace the ZO raypath down to reflector $N-1$, starting with emergence angle ψ_0 [relation (4)] at the surface, applying Snell's law at each interface, thus obtaining $\Delta T_1 \cdots \Delta T_{N-1}, \psi_1' \cdots \psi_{N-1}', \psi_1 \cdots \psi_{N-2}$.
(4) Derive ΔT_N, ψ_{N-1}, c_N from relations (2b), (2c), and Snell's law at interface $N-1$ ($\sin\psi_{N-1}'/c_{N-1} = \sin\psi_{N-1}/c_N$).
(5) Having determined these three parameters, the Nth part of the ZO path is defined and the Nth reflector is positioned perpendicular to the end of the ZO path (normal incidence point).

For horizontally layered systems [$dT_N(0)/dx' = 0$ for all N] this method yields the same results as Dix's inversion formula

$$c_N^2 = \frac{C_N^2 T_N(0) - C_{N-1}^2 T_{N-1}(0)}{T_N(0) - T_{N-1}(0)}. \tag{5}$$

From the conventional methods mentioned in the Introduction, we selected Hubral's method because it is of interest for our wave-theoretical approach to velocity determination, as shown in the following sections.

EXAMPLE OF CONVENTIONAL VELOCITY DETERMINATION PROCEDURES

Before describing the theory, an example of conventional methods, applied to synthetic data, is given. Consider the dipping plane-layered system, shown in Figure 3a. From CMP data, as shown in Figure 3b, NMO velocities C_N and ZO traveltimes $T_N(0)$ can be derived for all N. Assuming the system is horizontally layered, interval velocities and layer thicknesses can be calculated, applying Dix's relation (5). Since the assumption is rather crude for the configuration, this method yields inaccurate results. More accurate results may be expected from Hubral's method. To determine reflector dips as well, time dips must be derived from ZO traveltimes from adjacent CMP gathers. In Table 1 the results of Dix's and Hubral's method are compared with the model values. It may be concluded that for the dipping plane-layer case Hubral's method yields significantly more accurate results than Dix's method.

INTRODUCTION TO THE WAVE-THEORETICAL APPROACH TO VELOCITY DETERMINATION

Now consider the layered system with arbitrarily curved interfaces shown in Figure 4. We assume we have already reconstructed layers 1 through $N-1$ (interval velocities and interface positions and curvatures are determined) and we want to determine the interval parameters of layer N. Interval velocity determination using Hubral's method as described in a previous section yields erroneous results since the interfaces are curved. Distortions in the hyperbolic traveltime/offset relation are due to two causes.

(1) Reflection by curved surface S_N. Because we make use of the CMP configuration this effect will be small, as the reflecting area, denoted by d in Figure 4, is small. In the following we will neglect this effect.
(2) Refraction through curved interfaces $S_1 \cdots S_{N-1}$. Particularly when offsets are not small this effect may influence the moveout curve significantly.

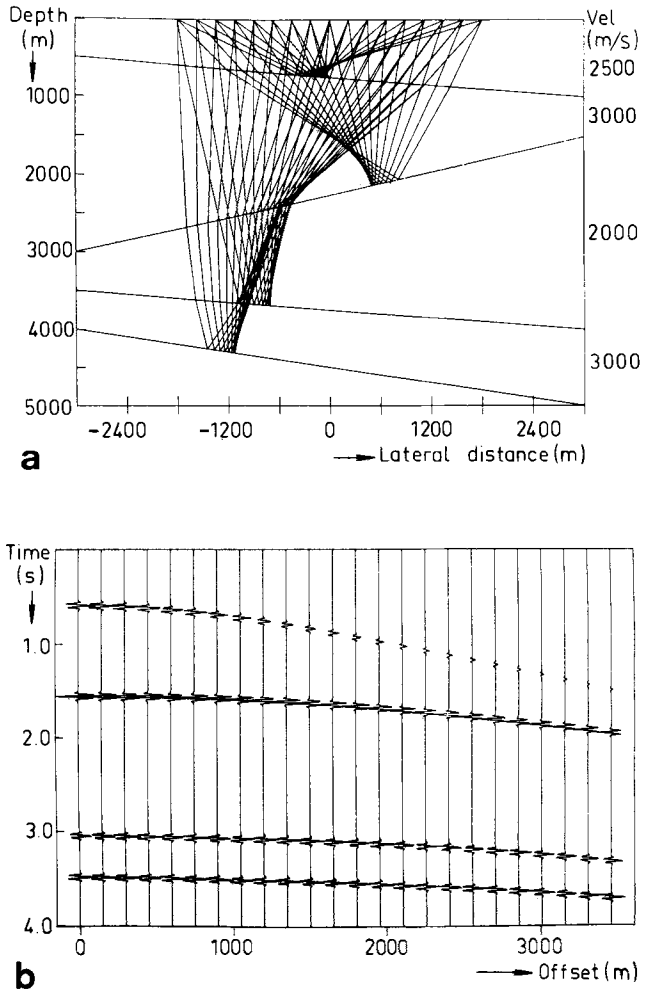

FIG. 3. Layered system with plane dipping interfaces: (a) subsurface with CMP rays, (b) CMP time series.

In the Introduction we mentioned that our method is based on application of conventional velocity determination techniques (Hubral's method) after preprocessing CMP gathers. We apply the VR process which is described in detail in the next section. Here we discuss the basic principle of our method. It is obvious that, when velocities $c_1 \cdots c_{N-1}$ are replaced by velocity c_N, the refraction effects of interfaces $S_1 \cdots S_{N-1}$ are eliminated even for wide offsets, since the inhomogeneous overburden is transformed into a homogeneous one. Hence, by means of VR, nonhyperbolic moveout curves are transformed into hyperbolic moveout curves. Since the replacement velocity c_N is unknown, an iterative method must be used. The initial estimate $\hat{c}_N$ can be obtained by applying Hubral's method to the original data, which are inaccurate because the interfaces are curved. Replacing $c_1 \cdots c_{N-1}$ by $\hat{c}_N$ yields a two-layer system with velocities $\hat{c}_N$ and c_N, respectively, as shown in Figure 5.

Table 1. Comparison of the results of Dix's and Hubral's method with the model values in the dipping plane-layer case. Since in Dix's method, horizontal layers are assumed, no dips are tabulated. (c = interval velocity, $|\Delta c/c|$ = relative error in c, Δz = layer thickness at common midpoint, α = reflector dip).

	Model			Dix			Hubral			
	c (m/s)	Δz (m)	α (deg)	c (m/s)	$\Delta c/c$	Δz (m)	c (m/s)	$\Delta c/c$	Δz (m)	α (deg)
1	2 500	750	4.8	2 508	0%	750	2 499	0%	750	4.8
2	3 000	1 500	−14.0	3 119	+4%	1 499	3 004	0%	1 502	−14.1
3	2 000	1 500	4.8	2 126	+6%	1 580	2 018	+1%	1 514	4.9
4	3 000	750	9.5	3 331	+11%	742	3 048	+2%	762	9.7

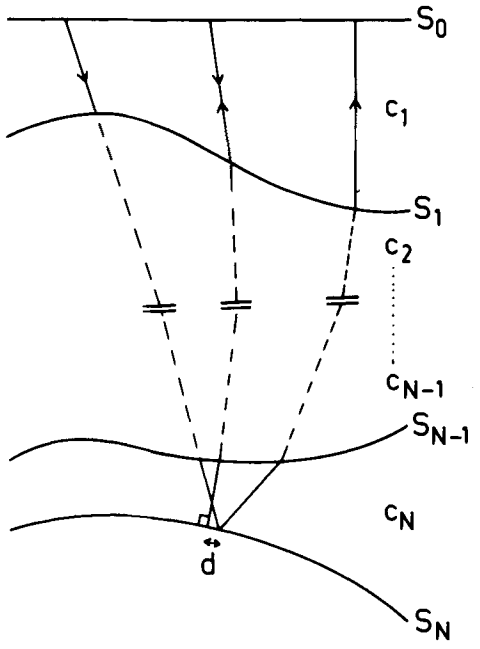

FIG. 4. Layered system with arbitrarily curved interfaces. For the CMP configuration the ZO ray and one wide offset ray for reflection N are shown.

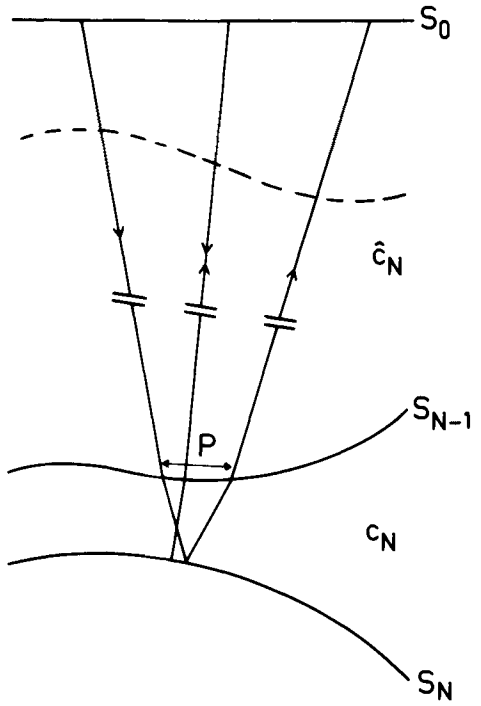

FIG. 5. Two-layer system which is obtained after replacing velocities $c_1 \cdots c_{N-1}$ of the system shown in Figure 4 by an estimate $\hat{c}_N$ of velocity c_N.

Application of Hubral's method to the two-layer system after VR in order to determine c_N will again yield erroneous results because interface S_{N-1} is curved.

However, three reasons why we may expect more accurate results from Hubral's method after VR than before VR follow.

(1) The inhomogeneous overburden (layers 1 through $N-1$) is replaced by a constant velocity medium, hence the refraction effects of curved interfaces $S_1 \cdots S_{N-2}$ are eliminated,
(2) Although $\hat{c}_N$ is not equal to c_N, generally the velocity discontinuity at interface S_{N-1} decreases when c_{N-1} is replaced by $\hat{c}_N$ (compare Figure 4 with Figure 5), and
(3) Particularly when the thickness of layer N is small, the refraction effects of interface S_{N-1} will be small since the refracting area, denoted by p in Figure 5, is small.

We conclude that application of Hubral's method after VR yields a new estimate $\hat{c}_N$ of the interval velocity of layer N. This value represents a more accurate estimate of the replacement velocity. The process can be repeated, which means c_N is determined iteratively. Theoretically, convergence is difficult to prove. However, many experiments with synthetic data, modeled under a wide range of subsurface conditions, have always shown convergence. Generally, application of two or three iteration steps per layer yields sufficient accuracy, although significant improvement of accuracy occurs already after one iteration step.

As seen in the dipping plane-layer case discussion, the following parameters can be determined from surface measurements: interval velocity, reflector depth, and reflector dip. Now we are dealing with layered systems with curved interfaces; hence application of Hubral's method to one CMP gather after VR yields the local interval velocity, the local reflector depth, and the local reflector dip for one normal incidence point. Application of the complete process (VR and Hubral) for several CMP gathers yields the parameters for several normal-incidence points. Optionally, the interval velocities may be laterally averaged. Finally, reflector S_N is reconstructed by interpolating cubic splines between the normal incidence points. Summarizing, based on the assumption that layers 1 through $N-1$ are reconstructed, we showed how layer N can be completely reconstructed.

VELOCITY REPLACEMENT

In our velocity determination procedure velocities in successive layers are replaced by one constant velocity. The replacement is achieved by wave field extrapolation of CMP data. In this section we describe this VR procedure. Consider the configuration shown in Figure 6. Assuming layers 1 through $N-1$ are reconstructed, VR for these layers is applied by (1) eliminating the propagation effects of layers 1 through $N-1$ (Figure 6a), and (2) simulating propagation effects for layers 1 through $N-1$ with one constant velocity $\hat{c}_N$ (Figure 6b). The elimination of the propagation effects of layers 1 through $N-1$ consists of $N-1$ inverse extrapolation steps of CMP data, the result of each step being a CMP gather recorded at a deeper interface. The final result after $N-1$ inverse

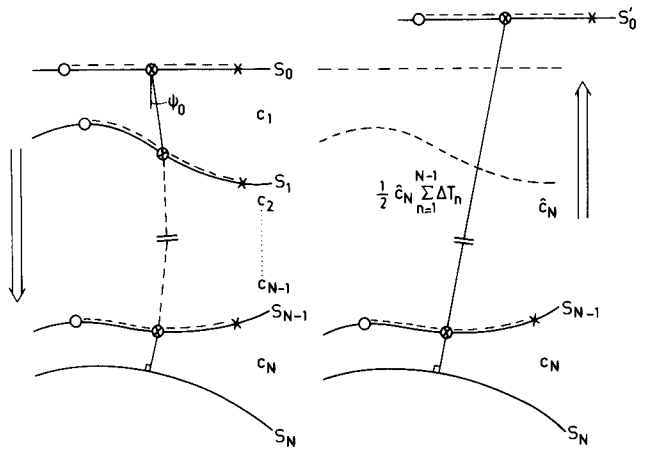

FIG. 6. Velocity replacement procedure: (a) elimination of inhomogeneous propagation effects, (b) simulation of homogeneous propagation effects.

extrapolation steps is a CMP gather recorded at interface $N-1$. The extrapolation algorithm for CMP data is described in the appendices.

Important parameters for each extrapolation step are the position and shape of two interfaces (begin and end situation for the specific extrapolation step) and the interval velocity between these interfaces. On the interfaces the sources and receivers are positioned equidistantly, centered on the midpoints. These midpoint locations can be calculated by tracing the ZO raypath down to reflector $N-1$, starting with emergence angle ψ_0 at the surface [which can be calculated from the time dip with the aid of relation (4)], applying Snell's law at each interface. The intersections of the ZO raypath with the interfaces indicate the midpoint positions. By choosing this extrapolation configuration the midpoint moves downward along the ZO raypath as a result of the inverse extrapolation. The ZO traveltime is reduced by ΔT_n in the nth extrapolation step, where ΔT_n represents the two-way interval traveltime of the ZO raypath in layer n. The total ZO traveltime reduction, as a result of $N-1$ inverse extrapolation steps, amounts to

$$\sum_{n=1}^{N-1} \Delta T_n.$$

Having performed $N-1$ inverse extrapolation steps, the underlying system is layer N with velocity c_N (see Figure 6a). Although we have reached the desirable situation of a CMP gather recorded over a homogeneous system (layer N), there are two reasons to complete the velocity replacement procedure by simulating propagation effects for layers 1 through $N-1$ with a forward extrapolation step, using replacement velocity $\hat{c}_N$.

(1) The recording surface (interface $N-1$) is curved, so the moveout curve is not hyperbolic.
(2) As a result of the extrapolation procedure boundary effects occur in the extrapolated CMP data, i.e., the hyperbolic moveout curve is distorted for large offsets, even when interface $N-1$ is plane. It is shown in Appendix C that these boundary effects can be suppressed for the greater part by the completion of the velocity replacement procedure with a forward extrapolation step (simulation of homogeneous propagation effects).

The simulation of the propagation effects for layers 1 through $N-1$ with one constant velocity $\hat{c}_N$ consists of one forward extrapolation step of CMP data, the result being a CMP gather recorded at the surface over a two-layer system with velocity $\hat{c}_N$ in the upper and c_N in the lower layer. The latter can be calculated rather accurately applying Hubral's method, as shown in the previous section. Since this forward extrapolation step is a simulation of propagation effects, we are free to choose the position and the shape of the surface. To obtain a hyperbolic moveout curve, we choose a plane surface. The position of the surface is determined by the ZO raypath. Since in the ideal situation $\hat{c}_N$ equals c_N, no ray deflection may occur at interface $N-1$ which determines the angle of the raypath. The length of the ZO raypath between the surface and interface $N-1$ we choose in such a way that the ZO traveltime reduction caused by the $N-1$ inverse extrapolation steps will be compensated, so this length amounts to

$$\frac{1}{2}\hat{c}_N \sum_{n=1}^{N-1} \Delta T_n.$$

The surface S'_0 is positioned at the end of this raypath parallel to the original surface S_0 (see Figure 6b). By choosing this extrapolation configuration, the ZO traveltime $T_N(0)$ does not change when the total VR procedure is applied. This means that the transformation of the CMP data (elimination of distortions in the moveout curve by means of elimination of the inhomogeneities in the system) is mainly restricted to the wide-offset data. When layer N is an inversion layer ($c_N < c_{N-1}$), then the position of the upper surface S'_0 after VR may be below the original surface S_0. In this case the hyperbolic moveout curve can only be retrieved within a smaller offset range due to boundary effects. On the other hand, when S'_0 is above S_0, the moveout curve will be available after VR for the complete offset range. Surface S'_0 will always be above S_0 when no inversion layers occur.

CMP TRACE INTERPOLATION

Before we show some examples, we briefly discuss a practical problem which is inherent to wave field extrapolation techniques. Because seismic data are discretized both in time and in space, two antialiasing criteria need be met (Berkhout, 1982)

$$\Delta t \leq \frac{1}{2f_{\max}},$$

and

$$\Delta s \leq \frac{\lambda_{\min}}{2 \sin \alpha_{\max}},$$

where

Δt = temporal sampling interval,
$f^{\max}$ = highest frequency,
Δs = spatial sampling interval (here, half-offset sampling interval),
$\lambda_{\min}$ = smallest wavelength,
and
$\alpha_{\max}$ = highest (raypath) dip angle.

Notice that λ_{min} should be related to half the propagation velocity (Appendix B), so $\lambda_{min} = \frac{1}{2}c_{min}/f_{max}$, where c_{min} is the lowest propagation velocity. In practical seismic acquisition techniques the first antialiasing condition is always fulfilled. However, in many situations spatial aliasing is inevitable due to spatial undersampling. As is well-known from signal theory, aliasing should be avoided by filtering before discretization. Only in special cases can antialiasing filtering be applied to discretized data. A crude but effective and widely applied procedure is muting large offsets at small traveltimes in CMP data. However, also relevant information may be suppressed by this procedure. Here we present an elegant approach to CMP trace interpolation, making use of prior information on the CMP gather.

NMO corrections applied to CMP data ideally transform all offset traces into zero-offset traces. In ideally NMO corrected CMP data, the dip angles have thus reduced to zero, which means that the second antialiasing condition is fulfilled for any discretization interval Δs. Now trace interpolation can be applied, yielding a new sampling interval $\Delta s' < \Delta s$. After an inverse ideal NMO correction, the interpolated CMP data are obtained, which are free of aliasing when $\Delta s'$ satisfies the second antialiasing condition. This procedure is only valid for CMP data, since the apices of all events lie on the same ZO trace, which is essential for NMO corrections. Also when the NMO corrections are not ideal, a significant reduction of the maximum dip angle will occur.

An example is presented in Figure 7. The CMP data of Figure 7a are undersampled by a factor of three. Applying one average NMO correction to the whole CMP data set (which simply involves time shifting of all traces) yields the result shown in Figure 7b. Notice that the steep dips have been reduced significantly. Application of an ideal interpolation in the wavenumber frequency domain yields the result shown in Figure 7c. (In practice, interpolation in the space-frequency domain is preferred, since it is faster and very good results can be obtained.) Finally, applying an inverse average NMO correction (again time shifting only) yields the interpolated CMP data, as shown in Figure 7d, with $\Delta s' = \Delta s/4$.

We discussed CMP trace interpolation because it is essential for our VR procedure. An additional advantage is that better resolved velocity spectra may be expected in conventional velocity analysis on aliasing free CMP gathers.

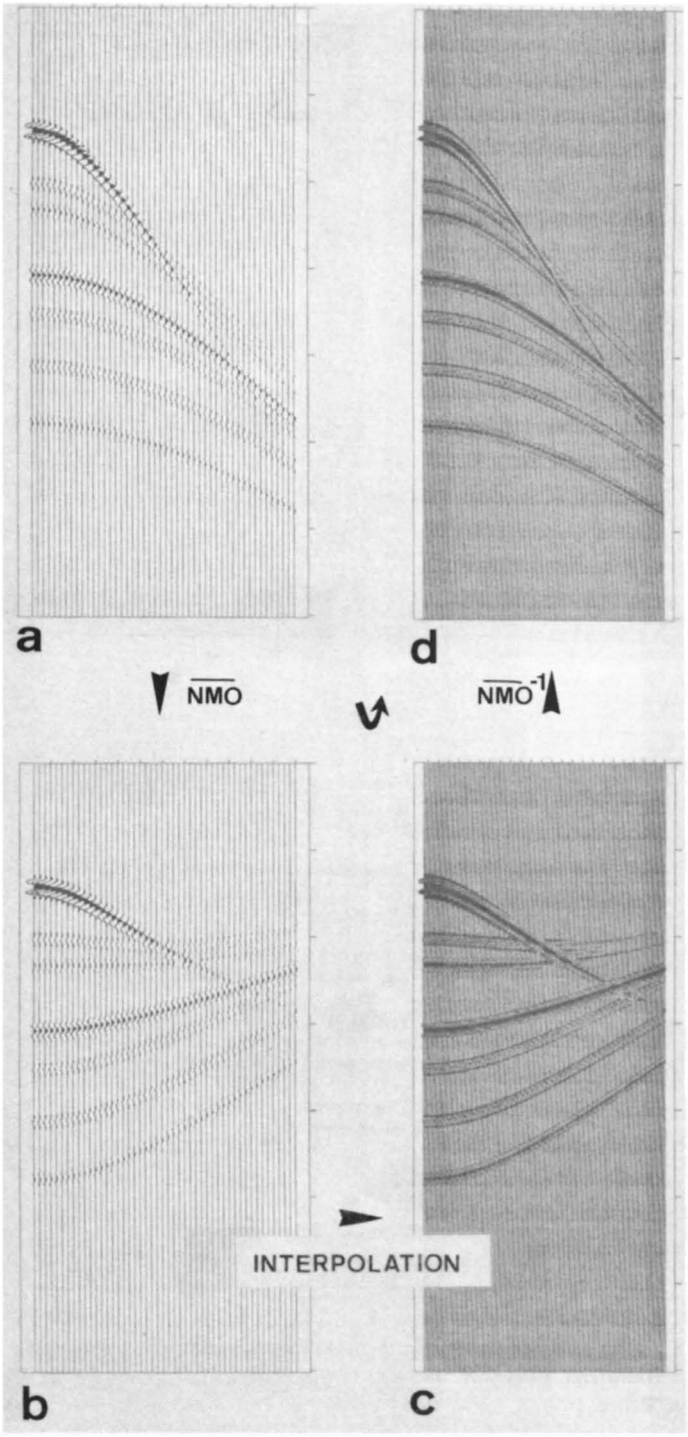

FIG. 7. CMP-trace interpolation: (a) undersampled CMP data, (b) correctly sampled CMP data after an average NMO correction, (c) oversampled NMO-corrected CMP data after trace interpolation, (d) correctly sampled CMP data after an inverse average NMO correction.

EXAMPLES OF VELOCITY DETERMINATION AFTER VELOCITY REPLACEMENT

In this section we discuss some results of the velocity determination procedure described in the previous sections, that is velocity determination after VR. In these examples we make use of synthetic data modeled with 2-D ray-tracing software. The data were modeled such that both the temporal and spatial antialiasing conditions were fulfilled. In the first example we show the results of the VR procedure applied to a layered system with arbitrarily curved interfaces. In the second example, a special application of the VR procedure is discussed, namely, elimination of near-surface anomalies.

(1) Layered system with arbitrarily curved interfaces

In this example we consider a layered system with arbitrarily curved interfaces as shown in Figure 8a. Before discussing the results obtained with velocity replacement, we show that conventional methods fail for this configuration. We modeled five CMP gathers from which NMO velocities and ZO traveltimes can be derived by means of coherence calculations. ZO time

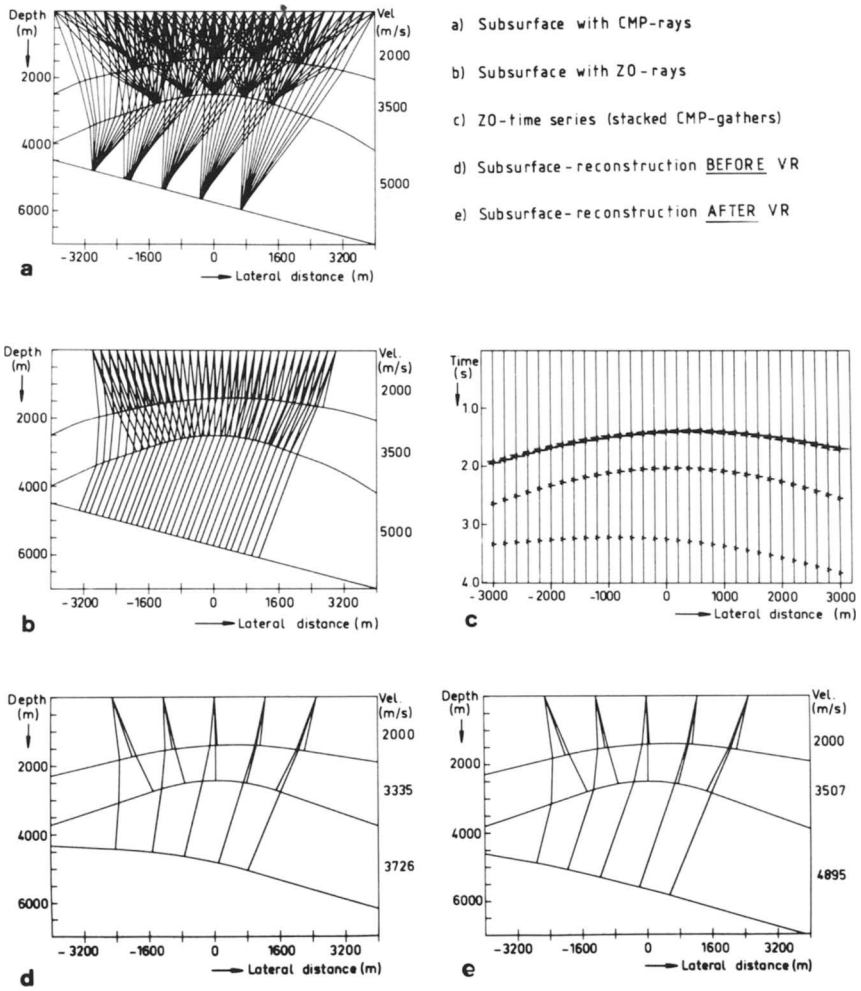

FIG. 8. Layered system with arbitrarily curved interfaces.

dips can be obtained from ZO data (in practice stacked CMP gathers), shown in Figures 8b and 8c. Since the interfaces are curved, the time dips vary laterally. For each of the five midpoint positions Hubral's method can be applied, assuming the interfaces are locally plane, thus obtaining local interval velocities, local reflector depths, and local reflector dips. Lateral averaging of the interval velocities yields the results shown in Table 2. Because curvature was ignored, up to 25 percent errors occurred. Interpolating cubic splines between the normal incidence points yields the subsurface configuration shown in Figure 8d. Notice that the third reflector, which is plane in the model (Figure 8a), is curved in the reconstruction as a result of the erroneous interval velocities.

We now discuss the VR procedure for this configuration. Since the system is homogeneous between the surface and the first interface, no VR is required to determine the interval parameters of the first layer. In the example described above, the first layer was indeed reconstructed correctly. In order to determine the interval parameters of layer 2 iteratively, the velocity c_1 in the first layer is replaced for one or more CMP gathers by an updated estimate $\hat{c}_2$ of the velocity in the second layer. As initial value we use $\hat{c}_2 = 3\ 335$ m/s, which was found by application of Hubral's method before VR. Since the velocity discontinuity at interface 1 after VR ($\hat{c}_2 = 3\ 335$ m/s, $c_2 = 3\ 500$ m/s) decreases compared to the discontinuity before VR ($c_1 = 2\ 000$ m/s, $c_2 = 3\ 500$ m/s), interval parameters of layer 2

Table 2. Comparison of the interval velocities obtained with Hubral's method before and after VR with the model values.

Model	Hubral before VR	Hubral after VR
$c_1 = 2\ 000$ m/s	$c_1 = 2\ 000$ m/s, $\Delta c_1/c_1 = 0\%$	$c_1 = 2\ 000$ m/s, $\Delta c_1/c_1 = 0\%$
$c_2 = 3\ 500$ m/s	$c_2 = 3\ 335$ m/s, $\Delta c_2/c_2 = -5\%$	$c_2 = 3\ 507$ m/s, $\Delta c_2/c_2 = 0\%$
$c_3 = 5\ 000$ m/s	$c_3 = 3\ 726$ m/s, $\Delta c_3/c_3 = -25\%$	$c_3 = 4\ 895$ m/s, $\Delta c_3/c_3 = -2\%$

are obtained more accurately applying Hubral's method after VR. A new updated estimate of $\hat{c}_2$ is obtained (after laterally averaging the velocity results of the different CMP gathers): $\hat{c}_2 = 3\,491$ m/s. This velocity is used as the replacement velocity in a new iteration step. Note again that the velocity inhomogeneity at interface 1 decreases ($\hat{c}_2 = 3\,491$ m/s, $c_2 = 3\,500$ m/s). When the desired accuracy for layer 2 is reached, interval parameters of layer 3 are determined in a similar way. Application of three iteration steps per layer and laterally averaging the velocity results of the different CMP gathers finally yield the results shown in Table 2. Notice that the accuracy increased significantly due to the application of VR. The error of 25 percent in c_3 has reduced to an error of 2 percent. The subsurface reconstruction is shown in Figure 8e. Notice that the third reflector is nearly plane, as in the original model (Figure 8a).

In this example we showed that the wave-theory based velocity determination procedure, as described here yields a complete reconstruction of a layered system with arbitrarily curved interfaces. Since for each layer VR has to be applied iteratively for one or more CMP gathers, this procedure is time-consuming compared to conventional methods. However, in the following example, a practical application is discussed where VR has to be applied for the surface layer only. The computation time for this example is comparable with the computation time needed for conventional methods.

(2) Elimination of near-surface anomalies

In marine as well as in land data nonhyperbolic moveout curves occur often as a result of near-surface anomalies. These anomalies are caused by a low-velocity surface layer (seawater, weathered earth layer, etc.) limited by a curved interface (seabottom, base of weathered layer, irregular topography). In practice, a correction is applied by means of a constant time shift (static correction). This approach is not optimal for offset data since one constant correction is applied for all depths which is obviously wrong. Application of velocity replacement is a wave-theoretical approach to the correction of near-surface anomalies. By replacing the irregular low-velocity layer by a layer whose velocity corresponds to the velocity in the next layer, the near-surface anomalies are eliminated correctly. We show this by comparing some important properties of the CMP data before and after VR. Consider the configuration shown in Figure 9a. This configuration represents a seawater layer (velocity $c_1 = 1\,500$ m/s) overlying horizontally layered sediments. The seabottom is represented by the first, curved interface. Although this restriction is not necessary, the sea level is represented by a plane surface. CMP data, as shown in Figure 9b, were modeled. To demonstrate the nonhyperbolic character of the moveout curves, the NMO velocities were calculated for two different offset ranges. The coherence of the NMO correct-

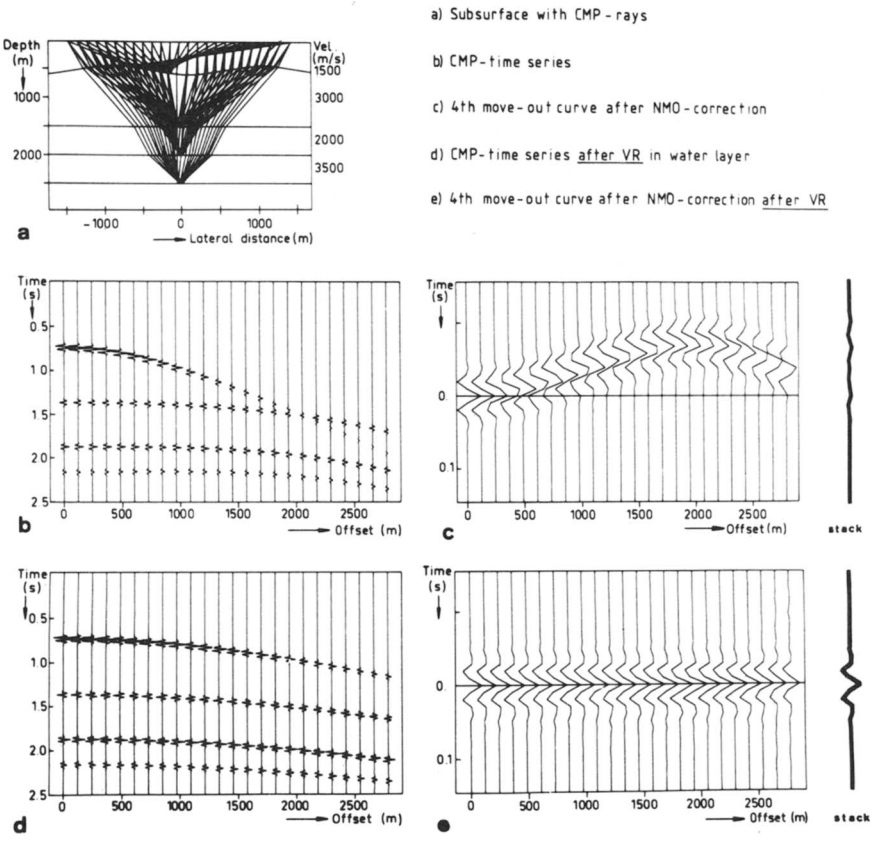

FIG. 9. Horizontally layered system overlain by a water layer with a curved seabottom.

Table 3: Some parameters derived from CMP data before VR. C = NMO-velocity, E = coherence of NMO-corrected traces, c = interval velocity, $\Delta c/c$ = relative error in c, $T(0)$ = ZO traveltime.

	Offset range (0→ 1 020) m	Offset range (0→ 2 760) m				Model
$T(0)$ (s)	C (m/s)	C (m/s)	E	c (m/s)	$\Delta c/c$	c (m/s)
.756	1 536	1 532	.595	1 532	+2%	1 500
1.380	3 788	2 532	.082	3 367	+12%	3 000
1.880	5 444	2 664	.070	2 998	+50%	2 000
2.166	∞	2 700	.056	2 926	−16%	3 500

ed traces was calculated for each moveout curve. The fourth moveout curve after NMO correction is shown in Figure 9c, together with the stacked trace. Finally the interval velocities were calculated according to Dix's relation (5). The results are shown in Table 3.

Because the curvature of the seabottom was ignored, the following observations can be made:

(1) the NMO velocities depend strongly on the offset range,
(2) the coherence of the NMO corrected traces is very low,
(3) the quality of the stacked trace is poor (Figure 9c), and
(4) errors up to 50 percent occur in the interval velocities.

Apparently the hyperbolic assumption for moveout curves 2, 3, and 4 is too crude in the case of near-surface anomalies.

By means of wave field extrapolation of the CMP data, the velocity in the first layer (c_1 = 1 500 m/s) is replaced by the velocity in the second layer (c_2 = 3 000 m/s). The layer thickness is adapted according to $\Delta z_{new} = (c_2/c_1)\Delta z_{old}$, so the ZO traveltimes are not influenced by the velocity replacement. The transformed CMP data are shown in Figure 9d. Note that the four moveout curves have undergone different transformations, which is a typical property of the wave-theoretical approach. The same calculations as before VR are applied to the transformed CMP data. The results are shown in Table 4, the fourth moveout curve after NMO correction is shown in Figure 9e, together with the stacked trace.

Due to the wave-theory based elimination of the velocity discontinuity at the seabottom, the following observations can be made:

(1) NMO velocities hardly depend on the offset range,
(2) coherence of the NMO-corrected traces is very good,
(3) quality of the stacked trace is high (Figure 9e), and
(4) accuracy of the interval velocities increased significantly.

Obviously the nonhyperbolic moveout curves have been transformed into hyperbolic ones.

CONCLUSIONS

In this paper we discussed the success of conventional velocity determination procedures when based on approximating the complicated traveltime/offset relation by a simple two-term hyperbolic relation. This approximation is sufficiently accurate in case of plane-layered systems (not necessarily horizontally layered). Furthermore, we showed that conventional procedures fail in more complicated situations, such as layered systems with arbitrarily curved interfaces, since the hyperbolic approximation is too crude. We showed, with the aid of wave field extrapolation of CMP data (VR), that the system can be transformed into a constant velocity system for which the hyperbolic relation holds. Although the restriction is not fundamental, we assumed 2-D situations. We discussed two examples of the VR procedure applied to synthetic data. In the first example the VR procedure was applied to data modeled in a system with arbitrarily curved interfaces. This example illustrates that application of the velocity determination procedure using VR yields significantly more accurate results than conventional methods. In the second example we discussed a special application, namely elimination of near-surface anomalies by means of VR in the surface layer. The result is a CMP gather without distortions caused by near-surface anomalies. The advantages are

Table 4. Some parameters derived from CMP data after VR: C = NMO-velocity, E = coherence of NMO-corrected traces, c = interval velocity, $\Delta c/c$ = relative error in c, $T(0)$ = ZO-traveltime. (The values in parentheses represent the replaced layer).

	Offset range (0 → 1 020) m	Offset range (0→ 2 760) m				Model
$T(0)$ (s)	C (m/s)	C (m/s)	E	c (m/s)	$\Delta c/c$	c (m/s)
(.756)	(3 020)	(3 016)	(.865)	(3 016)	(+1%)	(3 000)
1.380	3 024	3 016	.993	3 016	+1%	3 000
1.880	2 808	2 800	.992	2 091	+5%	2 000
2.166	2 952	2 932	.986	3 684	+5%	3 500

(1) Application of conventional velocity analysis methods after elimination of the near-surface anomalies by means of VR yields significantly more accurate results than velocity determination on the original data.
(2) The nonhyperbolic moveout curves have been transformed into *hyperbolic* curves, which improves the quality of the stacked data significantly.

ACKNOWLEDGMENTS

The authors are very grateful to GeoQuest Int. Ltd., Houston, Texas, for their financial support and for their permission to publish this paper. Also the help of Jos Kokke is greatly appreciated. He developed the CMP trace interpolation software as part of his M.Sc. project.

REFERENCES

Berkhout, A. J., 1982, Seismic Migration: Elsevier Scientific Publ. Co.
Cook, E. E., 1967, Geophysical reconnaissance in the Northwestern Caribbean: Presented at 37th Annual International SEG meeting, Oklahoma City, October 31.
De Vries, D., and Berkhout, A. J., 1982, Minimum entropy as a tool for velocity analysis: Presented at 52nd Annual International SEG meeting, Dallas, October 19.
Diebold, J. B., and Stoffa, P. L., 1981, The traveltime equation, tau-p mapping, and inversion of common midpoint data: Geophysics, **46**, 238–254.
Dix, C. H., 1955, Seismic velocities from surface measurements: Geophysics, **20**, 68–86.
Doherty, S. M., and Claerbout, J. F., 1976, Structure independent velocity estimation: Geophysics, **41**, 850–881.
Durbaum, H., 1954, Zur Bestimmung von Wellengeschwindigkeiten aus reflexion seismischen Messungen: Geophys. Prosp., **3**, 151–167.
Gardner, G. H. F., French, W. S., and Matzuk, T., 1974, Elements of migration and velocity analysis: Geophysics, **39**, 811–825.
Gjøystdal, H., and Ursin, B., 1981, Inversion of reflection times in three dimensions: Geophysics, **46**, 972–983.
Hubral, P., 1976, Interval velocities from surface measurements in the three-dimensional plane layer case: Geophysics, **41**, 233–242.
Krey, Th., 1976, Computation of interval velocities from common reflection point move-out times for n layers with arbitrary dips and curvatures in three dimensions when assuming small shot-geophone distances: Geophys. Prosp., **24**, 91 111.
Larner, K. L., and Rooney, M., 1972, Interval velocity computation for plane dipping multilayered media: Presented at 42nd Annual International SEG Meeting, Anaheim, California, November 30.
Lynn, W. S., and Claerbout, J. F., 1982, Velocity estimation in laterally varying media: Geophysics, **47**, 884–897.
May, B. T., and Straley, D. K., 1979, Higher order moveout spectra: Geophysics, **44**, 1193 1207.
Sattlegger, J. W., 1975, Migration velocity determination: Part I. Philosophy: Geophysics, **40**, 1–5.
Shah, P. M., 1973, Use of wavefront curvature to relate seismic data with subsurface parameters: Geophysics, **38**, 812–825.
Taner, M. T., and Koehler, F., 1969, Velocity spectra-digital computer derivation and applications of velocity functions: Geophysics, **34**, 859–881.
Tuchel, G., 1943, Seismische Messungen; Taschenbuch für Angewandte Geophysik: Leipzig.
Vander Made, P. M., Van Riel, P., and Berkhout, A. J., 1984, Velocity and subsurface geometry inversion by parameter estimation in complex inhomogeneous media: To be presented at 54th Annual International SEG Meeting, Atlanta, December.
Yilmaz, O., and Chambers, R. E., 1980, Velocity analysis by wavefield extrapolation: Presented at 50th Annual International SEG Meeting, Houston, November 19.

APPENDIX A
WAVE FIELD EXTRAPOLATION, GENERAL CONSIDERATIONS

In the velocity replacement section we showed that VR for layers 1 through $N-1$ is achieved by the performance of N ($N-1$ inverse and 1 forward) extrapolation steps of CMP data. In Appendix A we discuss some aspects of wave field extrapolation in general. In Appendix B wave field extrapolation of CMP data is dealt with as a special application. In Appendix C some properties of the VR procedure are discussed. To start a prestack forward extrapolation (continuation) scheme derived by Berkhout (1982) is explained. This extrapolation scheme can be elegantly represented by a matrix equation in the space-frequency domain for each single-frequency component. Forward extrapolation of a multirecord data set $\underset{\sim}{P}(S_{i+1})$ registered at plane, dipping surface S_{i+1} [for each source/receiver combination at S_{i+1} a registration is present in $\underset{\sim}{P}(S_{i+1})$] is applied by the matrix multiplication

$$\underset{\sim}{P}(S_i) = \underset{\sim}{W}(S_i, S_{i+1})\underset{\sim}{P}(S_{i+1})\underset{\sim}{W}(S_{i+1}, S_i), \qquad \text{(A-1a)}$$

the result being the extrapolated multirecord data set $\underset{\sim}{P}(S_i)$ registered at plane, dipping surface S_i. The forward restriction means that we are simulating the physical process of wave propagation. Element P_{mn} of data matrix $\underset{\sim}{P}$ represents the pressure, radiated by source n and registered by receiver m on the same surface. Column n represents the nth common source gather, row m the mth common receiver gather. The diagonals represent common offset gathers (main diagonal = ZO gather), the antidiagonals CMP gathers. $\underset{\sim}{W}(S_i, S_{i+1})$ and $\underset{\sim}{W}(S_{i+1}, S_i)$ represent forward extrapolation matrices for the receivers and sources, respectively. Relation (A-1a) is visualized in Figure A-1. As we assumed constant velocity sediments within the layers, we may define the matrices $\underset{\sim}{W}$ with the aid of the Rayleigh-II integral. Then their elements are given by

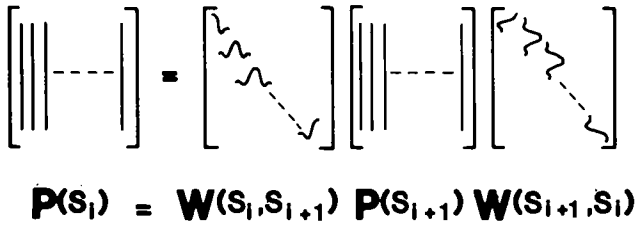

FIG. A-1. Schematic representation of wave field extrapolation of prestack data.

$$W_{mn}(S_i, S_{i+1}) = \sqrt{\frac{jk}{2\pi}} \cos \phi_{mn} \frac{e^{-jkr_{mn}}}{\sqrt{r_{mn}}} \Delta s \quad \text{for } kr_{mn} \gg 1,$$

and (A-1b)

$$W_{nm}(S_{i+1}, S_i) = \sqrt{\frac{jk}{2\pi}} \cos \phi'_{mn} \frac{e^{-jkr_{mn}}}{\sqrt{r_{mn}}} \Delta s \quad \text{for } kr_{mn} \gg 1,$$

where

$$k = 2\pi f/c,$$

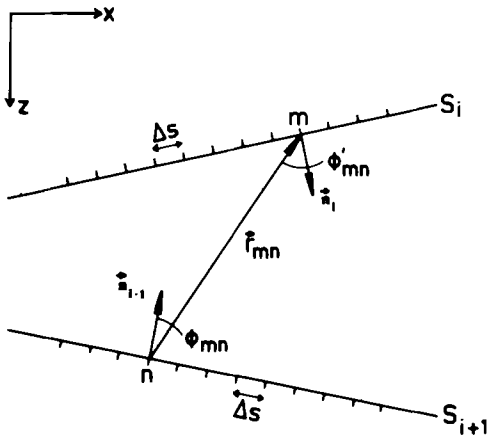

FIG. A-2. Extrapolation configuration.

with

k = wavenumber,
f = frequency,
c = propagation velocity,
r_{mn} = distance between position n on S_{i+1} and position m on S_i,
Δs = spatial sample interval,
ϕ_{mn} = angle between $\mathbf{r}_{mn}$ and normal $\mathbf{n}_{i+1}$ to surface S_{i+1},
ϕ'_{mn} = angle between $\mathbf{r}_{mn}$ and normal $\mathbf{n}_i$ to surface S_i,
and
j = imaginary unit ($\sqrt{j}$ is defined in the first quadrant).

(See Figure A-2.)

In case of no lateral variations (c constant, S_i is parallel to S_{i+1}), matrix $\underset{\sim}{\mathbf{W}}(S_i, S_{i+1})$ equals matrix $\underset{\sim}{\mathbf{W}}(S_{i+1}, S_i)$. In this case $\underset{\sim}{\mathbf{W}}$ is a Toeplitz matrix and relation (A-1a) is an alternative representation of spatial convolutions where the convolution operator W is space invariant. Berkhout (1982) shows that relation (A-1a) then can be transformed to the wavenumber-frequency domain where the convolutions are replaced by multiplications. In this domain the transformed operator $\tilde{\mathbf{W}}$ is given by

$$\tilde{\mathbf{W}} = \exp\left(-j\sqrt{k^2 - k_x^2}\,\Delta z\right) \qquad \text{for } k_x \le k,$$

and (A-1c)

$$\tilde{\mathbf{W}} = \exp\left(-\sqrt{k_x^2 - k^2}\,\Delta z\right) \qquad \text{for } k_x > k,$$

where

$$\Delta z = z_{i+1} - z_i > 0$$

with

Δz = distance between parallel surfaces S_{i+1} and S_i,
k = wavenumber,
and
k_x = Fourier equivalent of horizontal coordinate.

Although extrapolation in the wavenumber-frequency domain can only be applied in case of no lateral variations, we use relation (A-1c) in Appendix C to demonstrate an important property of the velocity replacement procedure.

To perform inverse extrapolation, $\underset{\sim}{\mathbf{P}}(S_{i+1})$ must be calculated from $\underset{\sim}{\mathbf{P}}(S_i)$ by means of inversion of relation (A-1a). Since inversion of matrices $\underset{\sim}{\mathbf{W}}$ is not stable, we choose the matched filter approach. Berkhout (1982) shows that band-limited inversion of relation (A-1a) can be approximated by

$$\underset{\sim}{\mathbf{P}}(S_{i+1}) = \underset{\sim}{\mathbf{F}}(S_{i+1}, S_i)\underset{\sim}{\mathbf{P}}(S_i)\underset{\sim}{\mathbf{F}}(S_i, S_{i+1}), \qquad \text{(A-2a)}$$

where

$$\underset{\sim}{\mathbf{F}}(S_{i+1}, S_i) = [\underset{\sim}{\mathbf{W}}^*(S_i, S_{i+1})]^T,$$

and

$$\underset{\sim}{\mathbf{F}}(S_i, S_{i+1}) = [\underset{\sim}{\mathbf{W}}^*(S_{i+1}, S_i)]^T. \qquad \text{(A-2b)}$$

Matrices $\underset{\sim}{\mathbf{F}}$ are obtained by transposition (T) and conjugation ($*$) of matrices $\underset{\sim}{\mathbf{W}}$. In case of no lateral variations the transpositions may be omitted. Relation (A-2a) then can be replaced by multiplications in the wavenumber-frequency domain, where the transformed operator $\tilde{F}$ is given by

$$\tilde{F} = \tilde{W}^*, \qquad \text{(A-2c)}$$

with $\tilde{W}$ defined by relation (A-1c).

In relations (A-1) and (A-2) we assumed that surfaces S_i and S_{i+1} are plane. By making this restriction we were able to derive an extrapolation scheme, based on the Raleigh-II integral. However, generally, surfaces S_i and S_{i+1} are curved and the extrapolation scheme must be derived from the Kirchhoff integral. The Rayleigh-II integral for plane surfaces is a special case of the Kirchhoff integral. Consider the Kirchhoff integral

$$P_A = \frac{1}{4\pi}\oint_S \left[P\,\frac{1+jkr}{r^2}\cos\phi e^{-jkr} + (j\omega\rho_0 V_n)\frac{e^{-jkr}}{r}\right] dS. \qquad \text{(A-3)}$$

This integral states that the pressure P_A in any point A inside a closed surface S can be calculated from a pressure dipole distribution P and a particle velocity monopole distribution V_n on S, provided that no sources are present inside S. Notice that both P and V_n on S yield the same frequency-dependent phase contribution $\exp(-jkr)$ to the pressure in A. Replacing P by $2P$ and deleting V_n yields the "Rayleigh-II integral for curved surfaces," with small amplitude errors only ($kr \gg 1$). Since in velocity analysis techniques the phase is far more important than the amplitude, application of the Rayleigh-II integral to curved surfaces is quite acceptable.

APPENDIX B
WAVE FIELD EXTRAPOLATION OF CMP DATA

In Appendix B we derive an algorithm for wave field extrapolation of CMP data, based on relation (A-1).

Consider relation (A-1a). The antidiagonals of data matrices $\underset{\sim}{\mathbf{P}}(S_i)$ and $\underset{\sim}{\mathbf{P}}(S_{i+1})$ represent one frequency component of the CMP gathers on (curved) surfaces S_i and S_{i+1}, respectively. In the extrapolation algorithm for CMP data we replace the data matrix $\underset{\sim}{\mathbf{P}}(S_{i+1})$ by a CMP gather by means of zeroing all off-antidiagonal elements, which is visualized in Figure B-1a.

Since we are only interested in the antidiagonal of matrix $\underline{\mathbf{P}}(S_i)$, the whole scheme can be reordered to

$$\mathbf{P}_{\mathrm{CMP}}(S_i) = \underline{\mathbf{T}}(S_i, S_{i+1})\mathbf{P}_{\mathrm{CMP}}(S_{i+1}), \tag{B-1a}$$

where $\mathbf{P}_{\mathrm{CMP}}(S_i)$ and $\mathbf{P}_{\mathrm{CMP}}(S_{i+1})$ are data vectors, representing the CMP gathers on S_i and S_{i+1}, respectively:

$$\mathbf{P}_{\mathrm{CMP}}(S_i) = [P_{-K,K} \cdots P_{0,0} \cdots P_{K,-K}]^T_{S_i}, \tag{B-1b}$$

and

$$\mathbf{P}_{\mathrm{CMP}}(S_{i+1}) = [P_{-K,K} \cdots P_{0,0} \cdots P_{K,-K}]^T_{S_{i+1}}, \tag{B-1c}$$

while $\underline{\mathbf{T}}(S_i, S_{i+1})$ represents the wave field extrapolation operator for CMP data. The reordered scheme is visualized in Figure B-1b. In order to derive operator $\underline{\mathbf{T}}$, we drop the matrix notation for a while. We rewrite relation (A-1a) as follows:

$$P_{mr}(S_i) = \sum_{n=-K}^{K} \sum_{\ell=-K}^{K} W_{mn}(S_i, S_{i+1}) P_{n\ell}(S_{i+1}) W_{\ell r}(S_{i+1}, S_i). \tag{B-1d}$$

Zeroing all off-antidiagonal elements of $\underline{\mathbf{P}}(S_{i+1})$, i.e., $P_{n\ell}(S_{i+1}) = 0$ when $n \neq -\ell$, yields the following expression for the antidiagonal elements of $\underline{\mathbf{P}}(S_i)$:

$$P_{m,-m}(S_i) = \sum_{n=-K}^{K} T_{mn}(S_i, S_{i+1}) P_{n,-n}(S_{i+1}), \tag{B-1e}$$

with

$$T_{mn}(S_i, S_{i+1}) = W_{mn}(S_i, S_{i+1}) W_{-n,-m}(S_{i+1}, S_i), \tag{B-1f}$$

or

$$T_{mn}(S_i, S_{i+1}) = \frac{jk}{2\pi} \cos \phi_{mn} \cos \phi'_{-m,-n} \frac{e^{-jk(r_{mn}+r_{-m,-n})}}{\sqrt{r_{mn} r_{-m,-n}}} \Delta s^2. \tag{B-1g}$$

From relation (B-1e), matrix relation (B-1a) follows immediately. Notice that the mth row of matrix $\underline{\mathbf{T}}(S_i, S_{i+1})$ is obtained by multiplying the individual elements of the mth row of matrix $\underline{\mathbf{W}}(S_i, S_{i+1})$ by the corresponding elements of the reversed column $-m$ of matrix $\underline{\mathbf{W}}(S_{i+1}, S_i)$, as is expressed by relation (B-1f).

In case of no lateral variations, relation (B-1g) can be simplified to

$$T_{mn}(S_i, S_{i+1}) = \frac{jk}{2\pi} \cos^2 \phi_{mn} \frac{e^{-2jkr_{mn}}}{r_{mn}} \Delta s^2. \tag{B-1h}$$

Notice that for this situation CMP-operator $\underline{\mathbf{T}}(S_i, S_{i+1})$ equals the ZO extrapolation operator, which is often approximated by $\underline{\mathbf{W}}(S_i, S_{i+1})$ as defined by (A-1b), with c replaced by $c/2$ (Berkhout, 1982). Now extrapolation algorithm (B-1a) can be replaced by a multiplication in the wavenumber-frequency domain

$$\tilde{P}_{\mathrm{CMP}}(S_i) = \tilde{T}(S_i, S_{i+1}) \tilde{P}(S_{i+1}), \tag{B-1i}$$

with

$$\tilde{T}(S_i, S_{i+1}) = \tilde{W}(S_i, S_{i+1}), (c \rightarrow c/2), \tag{B-1j}$$

where $\tilde{P}_{\mathrm{CMP}}$ denotes the spatial Fourier transform of $\mathbf{P}_{\mathrm{CMP}}$, while $\tilde{W}$ was already defined in relation (A-1c).

To describe inverse extrapolation of CMP data, we again use the matched filter approach

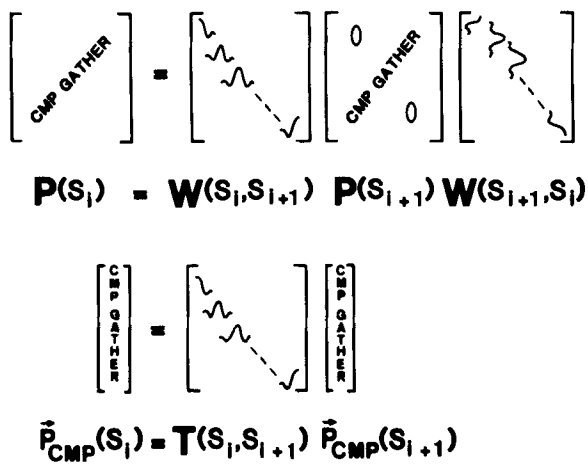

FIG. B-1. Schematic representation of wave field extrapolation of CMP data: (a) Data reduction, (b) reordering.

$$\mathbf{P}_{\mathrm{CMP}}(S_{i+1}) = \underline{\mathbf{X}}(S_{i+1}, S_i)\mathbf{P}_{\mathrm{CMP}}(S_i), \tag{B-2a}$$

where

$$\underline{\mathbf{X}}(S_{i+1}, S_i) = [\underline{\mathbf{T}}^*(S_i, S_{i+1})]^T. \tag{B-2b}$$

In case of no lateral variations the transposition can be omitted and algorithm (B-2a) can be replaced by a multiplication in the wavenumber-frequency domain

$$\tilde{P}_{\mathrm{CMP}}(S_{i+1}) = \tilde{X}(S_{i+1}, S_i)\tilde{P}_{\mathrm{CMP}}(S_i), \tag{B-2c}$$

where

$$\tilde{X}(S_{i+1}, S_i) = \tilde{T}^*(S_i, S_{i+1}). \tag{B-2d}$$

Of course, in situations where VR need be applied (such as curved interfaces), expressions (B-1h) through (B-1j) and (B-2c) and (B-2d) cannot generally be used.

DISCUSSION

Ideally, prestack wave field extrapolation should be applied to data matrices $\underline{\mathbf{P}}$ by means of relation (A-1a), which follows directly from wave theory. Velocity analysis should then be applied to data vectors $\mathbf{P}_{\mathrm{CMP}}$, which can be selected from matrices $\underline{\mathbf{P}}$. The method that we proposed in this paper involves a significant reduction of computational effort since both wavefield extrapolation and velocity analysis are applied to data vectors $\mathbf{P}_{\mathrm{CMP}}$. Of course errors are introduced by neglecting all off-antidiagonal elements in matrices $\underline{\mathbf{P}}$. However, we showed that for horizontally layered media (no lateral variations) the CMP operator equals the ZO operator. Since for this situation CMP-reflection data equal ZO diffraction data (apart from amplitude effects), it means that the algorithm (B-1a) is correct in spite of the simplification. Theoretically, the accuracy of the scheme decreases when the interface dips or curvatures increase. However, errors can be reduced to a minimum when the midpoint follows the ZO raypath in all extrapolation steps, as demonstrated with the numerical examples.

Note that conventional stacking may be considered as a nonrecursive migration process (diffraction stack version) along the ZO raypath.

APPENDIX C
SOME PROPERTIES OF THE VELOCITY REPLACEMENT PROCEDURE

In Appendix C we study some specific advantageous properties of the VR procedure. VR can be performed by means of $N-1$ inverse and one forward extrapolation step of CMP data, which can be represented by the following matrix multiplication

$$\mathbf{P}_{\mathrm{CMP}}(S_0') = \underset{\sim}{\mathbf{T}}(S_0', S_{N-1})\underset{\sim}{\mathbf{X}}(S_{N-1}, S_{N-2}) \cdots \underset{\sim}{\mathbf{X}}(S_{i+1}, S_i) \cdots \times \underset{\sim}{\mathbf{X}}(S_1, S_0)\mathbf{P}_{\mathrm{CMP}}(S_0) \quad \text{(C-1a)}$$

where $\mathbf{P}_{\mathrm{CMP}}(S_0)$ represents the original CMP data set at the acquisition surface S_0 and where $\mathbf{P}_{\mathrm{CMP}}(S_0')$ represents the CMP data set after velocity replacement at the new surface S_0'. (In the velocity replacement section we showed that S_0 and S_0' do not necessarily coincide.) For the moment we consider the simplified situation of a horizontally layered system, which means that relation (C-1a) represents a number of spatial space-invariant convolutions. So for this simplified situation VR can be performed in the wavenumber-frequency domain by means of the following simple scalar multiplication (see also Appendices A and B)

$$\tilde{P}_{\mathrm{CMP}}(S_0') = \exp\left(-j\sqrt{\bar{k}^2 - k_x^2}\,\Delta\bar{z}\right)\prod_{i=1}^{N-1}\left[\exp\left(+j\sqrt{k_i^2 - k_x^2}\,\Delta z_i\right)\right] \times \tilde{P}_{\mathrm{CMP}}(S_0), \quad \text{for } |k_x| < k_i, \quad \forall i, \quad \text{(C-1b)}$$

where

$$k_i = \frac{2\pi f}{c_i/2},$$

$$\bar{k} = \frac{2\pi f}{\bar{c}/2},$$

$$\Delta z_i = z_i - z_{i-1} > 0,$$

and

$$\Delta\bar{z} = z_{N-1} - z_0' > 0,$$

with

c_i = interval velocity in layer i,
$\bar{c}$ = replacement velocity (in practice we use $\bar{c} = \hat{c}_N$, which is an estimate of c_N),
z_i = depth coordinate of surface S_i,
and
z_0' = depth coordinate (pos. or neg.) of surface S_0'.

We leave the evanescent field ($|k_x| > k_i$) out of consideration. Note that the $c/2$ substitution has been used. For $|k_x| \ll \bar{k}$ and $|k_x| \ll k_i$, relation (C-1b) can be approximated by the following equation

$$\tilde{P}_{\mathrm{CMP}}(S_0') = \exp\left[j\left\{\sum_{i=1}^{N-1}(k_i\Delta z_i) - \bar{k}\Delta\bar{z}\right\}\right] \times \exp\left[-j\frac{k_x^2}{2}\left\{\sum_{i=1}^{N-1}(\Delta z_i/k_i) - \Delta\bar{z}/\bar{k}\right\} + O(k_x^4)\right]\tilde{P}_{\mathrm{CMP}}(S_0). \quad \text{(C-1c)}$$

In the velocity replacement section we defined the replacement step size $\Delta\bar{z}$ by

$$\Delta\bar{z} = \tfrac{1}{2}\hat{c}_N\sum_{i=1}^{N-1}\Delta T_i = \frac{1}{\bar{k}}\sum_{i=1}^{N-1}k_i\Delta z_i.$$

By substituting this relation for $\Delta\bar{z}$ in relation (C-1c) the argument of the first exponent in (C-1c) equals zero. In this case relation (C-1c) represents a phase shift depending on k_x^2 which equals zero for $k_x^2 = 0$ and which increases for increasing k_x^2. Translated to the (x, t) domain it means that the ZO traveltime does not change, while the offset traces undergo an increasing time shift for increasing offset. This result was stated in the velocity replacement section. Consider the argument of the second exponent in relation (C-1c). The summation term is due to the $N-1$ inverse extrapolation steps, the term $\Delta\bar{z}/\bar{k}$ is due to the forward extrapolation step. Here the importance of the forward extrapolation step in the VR procedure becomes clear: it reduces the absolute value of the argument of the extrapolation operator in the wavenumber-frequency domain. Translated to the space-frequency domain this means that the convolution operator width in relation (C-1a) is reduced due to the replacement step, which is advantageous with respect to boundary effects. In the situation that $c_1 = c_2 = \cdots = c_{N-1} = \bar{c}$ relation (C-1c) can be replaced by

$$\tilde{P}_{\mathrm{CMP}}(S_0') = 1 \cdot \tilde{P}_{\mathrm{CMP}}(S_0), \quad \text{(C-1d)}$$

where surface S_0' equals surface S_0. The equivalence of this relation in the space-frequency domain is a convolution of $\mathbf{P}_{\mathrm{CMP}}(S_0)$ with a band-limited spatial δ-pulse, which means in this case that our VR algorithm (C-1a) is exact within the spatial bandwidth.

In Appendix B we showed that forward wave field extrapolation of CMP data can be performed by means of matrix multiplication (B-1a), inverse extrapolation is described by relation (B-2a). Application of each individual extrapolation step yields boundary effects as a result of the finite operator width. However, in Appendix C we show, by means of evaluation of matrix equation (C-1a), that for a horizontally layered system these boundary effects are suppressed for the greater part, when VR is carried out. We also showed that for a special case ($c_1 = c_2 = \cdots = c_{N-1} = \bar{c}$) relation (C-1a) is exact within the spatial bandwidth.

The above properties of the VR procedure are also valid for systems with curved interfaces. However, since we are dealing here with lateral variations, the wavenumber-frequency domain cannot be used anymore. Because the argumentation in the space-frequency domain is far more complicated, the above properties are demonstrated here with the numerical examples.